Mathematical Biosciences and Engineering

https://www.aimspress.com/journal/mbe

MBE, 23(4): 1067–1095.
DOI: 10.3934/mbe.2026040
Received: 17 July 2025
Revised: 21 December 2025
Accepted: 30 January 2026
Published: 09 March 2026

Research article

Mathematical modeling of the effects of screening and treatment of gastric ulcers as a control strategy for gastric cancer

Glory Kawira Mutua[1,*], **Musyoka Kinyili**[1,2] **and Dominic Makaa Kitavi**[1,3]

[1] Department of Mathematics and Statistics, University of Embu, Kenya

[2] School of Computer Science and Applied Mathematics, University of the Witwatersrand, Johannesburg, South Africa

[3] College of Computer Studies, De La Salle University, Philippines

* **Correspondence:** Email: kawira.glory@embuni.ac.ke.

Abstract: Gastric cancer is among the most common cancers in the world, and it has a significant negative impact on the health and economies of different countries, led by those that are developing. This study formulates a deterministic model for the transmission dynamics of gastric cancer through gastric ulcers, incorporating screening and treatment strategies. The model is thoroughly analyzed both quantitatively, qualitatively, and numerically. The key properties considered in the model analysis are positivity, invariant region, equilibria, stabilities, and bifurcation analysis. We compute the control reproduction number $\mathcal{R}_C$ using the next-generation matrix approach. This enables us to prove that the model has a unique disease-free equilibrium (DFE) and admits a unique endemic equilibrium, which are locally and globally asymptotically stable whenever $\mathcal{R}_C < 1$ and $\mathcal{R}_C > 1$, respectively. Sensitivity analysis indicates that increasing the rate of screening decreases the control reproduction number, consequently reducing the rate of transmission of infections. Simulation results demonstrate that the combination of screening and treatment is the most effective intervention in reducing infection transmission. Furthermore, a combination of early screening and treatment proves more effective than a combination of late screening and treatment of gastric ulcers. Screening the infected population alone is identified as the least effective strategy for curtailing transmission of infection in the susceptible population. The findings of this study will guide public health officers in making decisions regarding the screening and treatment of exposed individuals with *Helicobacter pylori* infection and gastric ulcer patients, therefore aiding in fighting gastric ulcers and their progression to gastric cancer.

Keywords: gastric cancer; gastric ulcers; mathematical modeling; control reproduction number; deterministic models; numerical simulations

1. Introduction

Gastric cancer (GC) has claimed and continues to claim many lives globally, taking close to one million lives every year [1]. GC is the fourth most common cause of cancer-related mortality globally [2]. For instance, in 2020, there were 1,089,103 cases of GC worldwide and claimed 768,793 lives [1]. This mortality rate is very high despite the availability of intervention strategies to curb its spread. About 90% of the individuals with gastric cancer are diagnosed at a late stage due to poor routine screening and inadequate understanding of the underlying mechanism [3]. Therefore, there is a need for thorough and intense innovation and research in controlling the transmission of the disease worldwide.

Helicobacter pylori (*H. pylori*) is the leading risk factor for gastric ulcers and gastric cancer [4]. It is a spiral-shaped, microaerophilic gram-negative bacterium categorized as a class I carcinogen in 1994 by the World Health Organization (WHO) [5]. *H. pylori* infections are estimated to infect about 50% of the world's population. Australian scientists Barry Marshall and Robin Warren identified *H. pylori* in 1982 [3]. In their work with human stomach specimens, *H. pylori* was shown to be the leading cause of gastric ulcers, duodenal ulcers, and chronic gastritis.

Gastric ulcers are open sores in the upper region of the digestive system that can cause stomach upset and stomach pain, leading to internal bleeding. It is a prevalent disease that affects millions of people around the world [6]. The WHO reports that 85,487 deaths in India were due to gastric ulcer disease, accounting for 0.96% of all deaths in India [7]. According to Hwang et al. [8], 86 out of 2387 Gastric ulcer (GU) patients who had *H. pylori* infection developed Gastric cancer (GC), which translates to a 0.41% yearly incidence rate. On the other hand, only 35 out of 2098 Duodenum ulcers (DU) patients who had *H. pylori* infection developed GC, meaning that the yearly incidence rate was 0.11%. These statistics show that GU patients have a considerably greater incidence rate and relatively higher risk of developing GC than DU patients [8]. For individuals with gastric ulcers, *H. pylori* eradication may lower their chance of getting gastric cancer.

Mathematical modeling is a valuable tool that helps to understand the transmission and progression dynamics of many diseases as well as assess the impact of various control interventions [9]. Researchers have conducted comprehensive studies on the dynamics of *H. pylori* infection and its role, but several research gaps still exist. Current mathematical models, like Mutua et al. [10], formulated the modified compartmental model, which focused on treating *H. pylori* infection. Feng et al. [11] created Markov models to determine the cost-effectiveness of *H. pylori* screening and eradication therapy in an asymptomatic population in China. Shen et al. [4] developed a compartmental model based on gastric cancer and diagnoses using Markov Chain Monte Carlo techniques. Cousin et al. [12] developed a simple SEIR compartment model for the transmission dynamics of *Campylobacter* (*Helicobacter pylori*) in Ontario, Canada. The aspect of natural history of the infection, drug resistance, control measures, and progression to severe outcomes, such as gastric cancer, is mostly ignored in existing models. Furthermore, mathematical models exploring the impacts of screening and treatment of gastric ulcers as control strategies for gastric cancer are underexplored.

Therefore, this paper formulates a deterministic mathematical model to examine the role of screening and treatment in curbing gastric ulcers and, consequently, gastric cancer. The model uses a population-based compartmental structure to perform analysis using first-order nonlinear ordinary differential equations. We determine the models' qualitative behavior by investigating model positivity and boundedness, equilibria, reproduction number, and stability analysis. We conduct numerical sim-

ulations and sensitivity analysis with respect to parameters of interest to track the predictions of the model on the course of the disease over time.

The rest of the paper is organized as follows: Section 2 presents the model formulation, where the main assumptions are annotated, the model is described, and the equations are derived. Section 3 is devoted to model analysis pertaining to positivity, boundedness, equilibria, stabilities, reproduction number, and bifurcation analysis. Section 4 is dedicated to the numerical analysis, sensitivity analysis, and simulation. Lastly, section 5 gives the conclusion.

2. Model formulation

2.1. Main assumptions

The model is built under the following assumptions:

A1: Individuals who are neither screened nor treated against gastric ulcers are highly prone to developing gastric cancer.
A2: Age structure is not considered in the model.
A3: An individual may develop gastric cancer as a result of being severely infected with gastric ulcers, drug resistance, non-adherence to drug prescriptions, etc.
A4: The rate of gastric cancer formation from infected individuals with gastric ulcers and screened humans against gastric ulcers is equal.
A5: The shedding rate of bacteria from the individuals who are actively infected with gastric ulcers and humans who are screened against gastric ulcers is equal.
A6: There is no natural recovery from gastric ulcers.
A7: Gastric ulcers do not confer permanent immunity.
A8: There is no recovery from gastric cancer.

2.2. Model description and equations

The deterministic model considers the transmission dynamics of gastric cancer through gastric ulcers. The model divides the human population into six mutually exclusive classes and collects the bacterial population from the environment into one class. All the classes depend on time and are annotated as follows:

- Susceptible class $S(t) = S$: These are individuals who do not have the infection but are likely to get the infection in the future.
- Exposed class $E(t) = E$: These are individuals who are in the latent phase of the disease. This means that the *H. pylori* which is the causative agent of gastric ulcers, is in the latent state, meaning that the bacterium is present in the gastric mucosa but at such low levels, hence not actively replicating or being shed in sufficient quantities. Thus, at this state individuals may not transmit the infection. It is from this class that individuals develop gastric ulcers when the levels of the *H. pylori* are high due to continuous active replication.
- Gastric ulcers infected class $I(t) = I$: These are individuals who are actively infected with gastric ulcers and showing symptoms of the disease. They are unaware of their infection status, especially during the early stages of the disease. However, they may become aware of their infection status

actually at the late stage of the disease, probably when symptoms start appearing. Thus, unless they are screened early or late, they are unlikely to seek or receive treatment.

- Screened class $I_S(t) = I_S$: These are individuals who are screened against gastric ulcers. This screening takes place in the early stages, especially for exposed individuals, or in the late stages for individuals already infected with gastric ulcers. Thus, the individuals in this class are aware of their gastric ulcers status because they have already been diagnosed with the disease. Therefore, some of them immediately proceed for treatment against gastric ulcers, while others develop gastric cancer as a result of late screening when the gastric ulcers has advanced to gastric cancer.
- Treatment class $T(t) = T$: These are the screened individuals who are undergoing treatment against gastric ulcers. Since gastric ulcers do not confer permanent immunity, a proportion of individuals receiving treatment against gastric ulcers fully recover and join the susceptible class. Another proportion of this class develops gastric cancer and progresses to class I_C mainly due to reasons such as drug resistance, nonadherence to drug prescriptions, etc.
- Gastric cancer infected class $I_C(t) = I_C$: These are individuals who suffer from gastric cancer as a result of severe complications from gastric ulcers.
- Bacteria class $B(t) = B$: This class represents the population of *H. pylori* in the environment.

Therefore, the model assumes that the total human population N at time t is given as

$$N(t) = S(t) + E(t) + I(t) + I_S(t) + T(t) + I_C(t). \tag{2.1}$$

H. pylori is mostly transmitted directly from an infectious human to a susceptible human [10]. In addition, bacteria can be transmitted by environmental factors, such as the use of contaminated water and food or coming into contact with contaminated surfaces [13]. Individuals in the infectious classes and the contaminated environment infect susceptible individuals $S(t)$, through the aforementioned modes of transmission. Thus, the force of infection for the model denoted by λ is given by

$$\lambda = \frac{\beta(I + \phi_1 I_s + \phi_2 T + \phi_3 I_c)}{N} + \frac{\nu B}{K + B}, \tag{2.2}$$

where; β denotes the effective contact rate for direct transmission. ϕ_1, ϕ_2, $\phi_3 < 1$ are the modification parameters which account for the infectiousness among individuals with infection of *H. pylori* in compartment I_S, T and I_C respectively, ν is the ingestion rate of *H. pylori* bacteria from the environment, K is the concentration of *H. pylori* bacteria causing half of the maximal environmental force of infection [14], and $\frac{B}{K+B}$ is the probability that ingesting an amount of *H. pylori* bacteria B results in infection [15, 16]. The susceptible individuals can get exposed to the infection at the rate λ, following effective contact with the infectious individual(s) and infection rate of the *H. pylori* bacteria from the environment. The model assumes that individuals can recover and join the $S(t)$ class (at the rate of ζ). The class is increased by recruitment at a rate π. Furthermore, the model assumes that individuals from all the classes die naturally at the rate μ. Thus, the rate of change of the susceptible class is given as

$$\frac{dS}{dt} = \pi + \zeta T - (\lambda + \mu)S. \tag{2.3}$$

The class $E(t)$ is increased by the force of infections λ when the susceptible individuals are exposed to the infection either through contact with the infectious individuals or when exposed to *H. pylori*

bacteria in the environment. Individuals in this class may come out being screened at the rate ω or join the gastric ulcers individuals at the rate ρ. The class is further decreased by the natural death rate μ, so that

$$\frac{dE}{dt} = \lambda S - (\omega + \mu + \rho)E. \tag{2.4}$$

The infected gastric ulcers class $I(t)$, is increased by individuals from $E(t)$ class at the rate ρ. The class declines by natural death rate μ, screening of the infected gastric ulcer individuals (at the rate θ), and infected individuals with gastric ulcers who develop gastric cancer directly at the rate α. So that

$$\frac{dI}{dt} = \rho E - (\theta + \alpha + \mu)I. \tag{2.5}$$

The screened class is increased by the individuals who have undergone medical screening from $E(t)$ class (at the rate ω) and $I(t)$ class (at the rate θ). The screened individuals can either join the class $T(t)$ undergoing treatment at the rate ϵ or develop gastric cancer at the rate of γ. We note that based on the assumption **A4**, $\gamma = \alpha$. The class is further reduced by the natural death rate μ. So that

$$\frac{dI_s}{dt} = \omega E + \theta I - (\mu + \epsilon + \gamma)I_S. \tag{2.6}$$

The class of individuals receiving treatment against gastric ulcers is increased by screened individuals who seek treatment at the rate of ϵ. However, since the model assumes that gastric ulcers do not confer permanent immunity, a proportion ζ of individuals receiving treatment against gastric ulcers fully recover and join the susceptible class $S(t)$. Another proportion η of the class $T(t)$ develops gastric cancer and progresses to the $I_C(t)$ class mainly due to reasons such as drug resistance, non-adherence to drug prescriptions, etc. This leads to the reduction of individuals in this class. Furthermore, the class is further reduced by individuals dying naturally at the rate of μ. Thus, the dynamics of this class are given by the equation

$$\frac{dT}{dt} = \epsilon I_S - (\mu + \eta + \zeta)T. \tag{2.7}$$

The class of gastric cancer is increased by infected individuals with gastric ulcers who develop gastric cancer without undergoing screening at the (rate α), screened individuals who may develop gastric cancer without treatment (at the rate γ, where, $\gamma = \alpha$ in accordance with assumption **A4**) and humans undergoing treatment who develop gastric cancer as a result of drug resistance in their body (at the rate η). The population declines by natural death rate μ and death due to gastric cancer, at the rate δ. Therefore

$$\frac{dI_C}{dt} = \alpha I + \gamma I_S + \eta T - (\mu + \delta)I_C. \tag{2.8}$$

The bacteria class $B(t)$ is increased by the shedding rates of the *H. pylori* bacteria from the environment by the infected class $I(t)$ (at the rate σ_1), screened class $I_S(t)$ (at the rate σ_2, where, $\sigma_2 = \sigma_1$ as

per the assumption **A5**), treated class $T(t)$ (at the rate σ_3) and infected gastric cancer class $I_C(t)$ (at the rate σ_4). Further, the model assumes that the bacteria die naturally at the rate τ. Thus, we have

$$\frac{dB}{dt} = \sigma_1 I + \sigma_2 I_S + \sigma_3 T + \sigma_4 I_C - \tau B. \tag{2.9}$$

The schematic representation of the Model (2.10) is given by **Figure 1** and the parameters values described in **Table 2.**

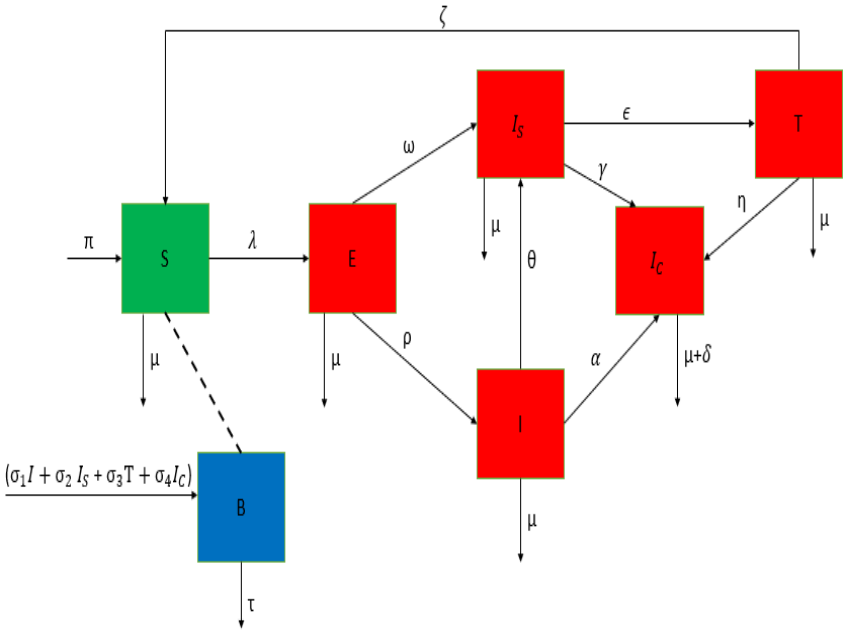

Figure 1. Schematic representation of the model. We note that, in line with assumptions **A4** and **A5**, $\gamma = \alpha$ and $\sigma_2 = \sigma_1$ respectively. This means that these parameters take equal values as captured later in Table 2.

Assembling equations (2.3)-(2.9) together, we have the model system of nonlinear ODEs as

$$\begin{cases} \frac{dS}{dt} &= \pi + \zeta T - (\lambda + \mu)S, \\ \frac{dE}{dt} &= \lambda S - (\omega + \mu + \rho)E, \\ \frac{dI}{dt} &= \rho E - (\theta + \alpha + \mu)I, \\ \frac{dI_s}{dt} &= \omega E + \theta I - (\mu + \epsilon + \gamma)I_S, \\ \frac{dT}{dt} &= \epsilon I_S - (\mu + \eta + \zeta)T, \\ \frac{dI_C}{dt} &= \alpha I + \gamma I_S + \eta T - (\mu + \delta)I_C, \\ \frac{dB}{dt} &= \sigma_1 I + \sigma_2 I_S + \sigma_3 T + \sigma_4 I_C - \tau B. \end{cases} \tag{2.10}$$

3. Model analysis

We analyze the basic model properties of the system (2.10) since the model tracks the human population. This activity is crucial, especially for preserving the model epidemiological significance [9].

3.1. Positivity and boundedness of the solution

In this subsection, we state and prove the following Lemmas, respectively, accounting for the positivity and boundedness of the solution of Model (2.10).

Lemma 3.1. *Let* $S(0) \geqslant 0$, $E(0) \geqslant 0$, $I(0) \geqslant 0$, $I_s(0) \geqslant 0$, $T(0) \geqslant 0$, $I_C(0) \geqslant 0$ *and* $B(0) \geqslant 0$. *Then the solution* $S(0) > 0$, $E(0) > 0$, $I(0) > 0$, $I_s(0) > 0$, $T(0) > 0$, $I_C(0) > 0$ *and* $B(0) > 0 \; \forall \; t \geqslant 0$.

Proof. Assume the solution of Model (2.10) is positive for all $t \geqslant 0$. Then, there exist a first time t^* such that $t^* = \inf\{t \mid S(t) = 0 \text{ or } E(t) = 0 \text{ or } I(t) = 0 \text{ or } I_S(t) = 0 \text{ or } T(t) = 0 \text{ or } I_C(t) = 0 \text{ or } B(t) = 0\}$. So that if $S(t^*) = 0$ then $\forall \; t \in \{0, t^*\}$, $S(0) > 0$, $E(0) > 0$, $I(0) > 0$, $I_s(0) > 0$, $T(0) > 0$, $I_C(0) > 0$ and $B(0) > 0$, $\dfrac{dS(t^*)}{dt} < 0$. Thus, from (2.3) $\dfrac{dS(t^*)}{dt} = \pi + \zeta T(t^*) > 0$ (Since the model parameters are defined to be positive), which contradicts the initial assumption that $\dfrac{dS(t^*)}{dt} < 0$. Similarly, following the same argument, it can be proved that $S(t)$, $E(t)$, $I(t)$, $I_S(t)$, $T(t)$, $I_C(t)$ and $B(t)\}$ are positive for all $t \geqslant 0$. □

Lemma 3.2. *Let*

$$\Omega = \left\{(S, E, I, I_S, T, I_C, B) \in \mathbb{R}^7_+ : 0 \leq N \leq \frac{\pi}{\mu}, \; 0 \leq B \leq \frac{(\sigma_1 + \sigma_2 + \sigma_3 + \sigma_4)\pi}{\tau\mu}\right\}$$

be a biological positive region defined for all $t \geqslant 0$. *Then, the region* Ω *is positively invariant and absorbing with respect to Model* (2.10).

Proof. First, we consider the equations representing the disease progression within the human compartments. So that, adding the first six equations in Model (2.10) yields,

$$\frac{dN}{dt} = \pi - \mu N - \delta I_C \leq \pi - \mu N. \tag{3.1}$$

Using integration factor technique and the Gronwall Inequality in [17] to solve equation (3.1) with $N(0) = N_0$, we obtain

$$N(t) \leq \frac{\pi}{\mu}(1 - e^{-\mu t}) + N_0 e^{-\mu t}. \tag{3.2}$$

By ODEs comparison theorem applied by [9] yields

$$\lim_{t \to \infty} \sup\{N(t)\} \leq \frac{\pi}{\mu}. \tag{3.3}$$

Thus, (3.2) and (3.3) show that the human population part of the Model (2.10) is bounded and attracting for all $t \geqslant 0$ [18]. As a result, the model solution is confined within the defined region. Similarly, considering the *H. pylori* bacteria concentration in the environment in (2.9), we have the results as

$$B(t) \leq \frac{(\sigma_1+\sigma_2+\sigma_3+\sigma_4)\pi}{\tau\mu} - B(0)\frac{(\sigma_1+\sigma_2+\sigma_3+\sigma_4)\pi}{\tau\mu}e^{-\tau t}. \tag{3.4}$$

So it follows that

$$\lim_{t\to\infty}\sup\{B(t)\} \leq \frac{(\sigma_1+\sigma_2+\sigma_3+\sigma_4)\pi}{\tau\mu}. \tag{3.5}$$

Therefore, the solution of Model (2.10) is positively invariant and attracting in the region Ω. □

3.2. Control reproduction number ($\mathcal{R}_C$)

We note that Model (2.10) has a disease-free equilibrium (DFE), which we denote and define as

$$\mathcal{E}^0 = \left(\frac{\pi}{\mu}, 0, 0, 0, 0, 0, 0\right). \tag{3.6}$$

The average number of secondary infections that result from a single infectious individual when introduced into a fully susceptible population is measured by the basic reproduction number [19]. The control reproduction number ($\mathcal{R}_C$) is the mean number of secondary infections sourced by a single infectious individual when introduced into a susceptible population where control measures are put in place [20]. To obtain $\mathcal{R}_C$, we use the next-generation matrix approach [21]. From the Model (2.10), $\mathcal{F}$ representing the secondary infections and $\mathcal{V}$ representing the transfer of infections are respectively given as

$$\mathcal{F} = \begin{pmatrix} \lambda S \\ 0 \\ 0 \\ 0 \\ 0 \\ 0 \end{pmatrix} \quad \text{and} \quad \mathcal{V} = \begin{pmatrix} (\omega+\mu+\rho)E \\ -\rho E + (\theta+\alpha+\mu)I \\ -\omega E - \theta I + (\mu+\epsilon+\gamma)I_S \\ -\epsilon I_S + (\mu+\eta+\zeta)T \\ -\alpha I - \gamma I_S - \eta T + (\mu+\delta)I_C \\ -\sigma_1 I - \sigma_2 I_S - \sigma_3 T - \sigma_4 I_C + \tau B \end{pmatrix}. \tag{3.7}$$

The transition matrices F and V are respectively the Jacobian matrices of $\mathcal{F}$ and $\mathcal{V}$ with respect to E, I, I_S, T, I_C and B, evaluated at the disease-free equilibrium $\mathcal{E}^0 = \left(\frac{\pi}{\mu}, 0, 0, 0, 0, 0, 0\right)$ as

$$F = \begin{pmatrix} 0 & \beta & \beta\phi_1 & \beta\phi_2 & \beta\phi_3 & \frac{\nu\pi}{K\mu} \\ 0 & 0 & 0 & 0 & 0 & 0 \\ 0 & 0 & 0 & 0 & 0 & 0 \\ 0 & 0 & 0 & 0 & 0 & 0 \\ 0 & 0 & 0 & 0 & 0 & 0 \\ 0 & 0 & 0 & 0 & 0 & 0 \end{pmatrix} \quad \text{and} \quad V = \begin{pmatrix} k_1 & 0 & 0 & 0 & 0 & 0 \\ -k_2 & k_3 & 0 & 0 & 0 & 0 \\ -\omega & -\theta & k_4 & 0 & 0 & 0 \\ 0 & 0 & -\epsilon & k_5 & 0 & 0 \\ 0 & -\alpha & -\gamma & -\eta & k_7 & 0 \\ 0 & -\sigma_1 & -\sigma_2 & -\sigma_3 & -\sigma_4 & \tau \end{pmatrix},$$

where,
$k_1 = \omega + \mu + \rho$, $k_2 = \rho$, $k_3 = \theta + \alpha + \mu$, $k_4 = \mu + \epsilon + \gamma$, $k_5 = \mu + \eta + \zeta$, and $k_7 = \mu + \delta$.
Finding the V^{-1}, we get

$$V^{-1} = \begin{pmatrix} \frac{1}{k_1} & 0 & 0 & 0 & 0 & 0 \\ \frac{k_2}{k_1k_3} & \frac{1}{k_3} & 0 & 0 & 0 & 0 \\ \frac{k_2\theta+k_3\omega}{k_1k_3k_4} & \frac{\theta}{k_3k_4} & \frac{1}{k_4} & 0 & 0 & 0 \\ \frac{\epsilon(k_2\theta+k_3\omega)}{k_1k_3k_4k_5} & \frac{\epsilon\theta}{k_3k_4k_5} & \frac{\epsilon}{k_4k_5} & \frac{1}{k_5} & 0 & 0 \\ \frac{N_1}{k_1k_3k_4k_5k_7} & \frac{N_2}{k_3k_4k_5k_7} & \frac{\epsilon\eta+k_5\gamma}{k_4k_5k_7} & \frac{\eta}{k_5k_7} & \frac{1}{k_7} & 0 \\ \frac{N_3}{k_1k_3k_4k_5k_7\tau} & \frac{N_4}{k_3k_4k_5k_7\tau} & \frac{N_5}{k_4k_5k_7\tau} & \frac{\eta\sigma_4+k_7\sigma_3}{k_5k_7\tau} & \frac{\sigma_4}{k_7\tau} & \frac{1}{\tau} \end{pmatrix},$$

with

$$\begin{aligned} N_1 &= \alpha k_2k_4k_5 + \epsilon\eta k_2\theta + \epsilon\eta k_3\omega + k_2k_5\gamma\theta + k_3k_5\gamma\omega, \\ N_2 &= \alpha k_4k_5 + \epsilon\eta\theta + k_5\gamma\theta, \\ N_3 &= \alpha k_2k_4k_5\sigma_4 + \epsilon\eta k_2\theta\sigma_4 + \epsilon\eta k_3\omega\sigma_4 + \epsilon k_2k_7\theta\sigma_3 + \epsilon k_3k_7\omega\sigma_3, \\ &\quad + k_2k_4k_5k_7\sigma_1 + k_2k_5\gamma\theta\sigma_4 + k_2k_5k_7\theta\sigma_2 + k_3k_5\gamma\omega\sigma_4 + k_3k_5k_7\omega\sigma_2, \\ N_4 &= \alpha k_4k_5\sigma_4 + \epsilon\eta\theta\sigma_4 + \epsilon k_7\theta\sigma_3 + k_4k_5k_7\sigma_1 + k_5\gamma\theta\sigma_4 + k_5k_7\theta\sigma_2, \\ N_5 &= \epsilon\eta\sigma_4 + \epsilon k_7\sigma_3 + k_5\gamma\sigma_4 + k_5k_7\sigma_2. \end{aligned}$$

Finding the spectra radius of FV^{-1}, we get the control reproduction number to be

$$\begin{aligned} \mathcal{R}_C &= \frac{1}{K\tau k_1k_3k_4k_5k_7}(\omega k_3(\frac{\pi}{\mu}\nu(k_7(k_5\sigma_2 + \epsilon\sigma_3) + (\epsilon\eta + k_5\gamma)\sigma_4) \\ &\quad + K\beta\tau(k_7(k_5\phi_1 + \epsilon\phi_2) + (\epsilon\eta + k_5\gamma)\phi_3)) + k_2(\frac{\pi}{\mu}\nu(k_7(k_5(k_4\sigma_1 \\ &\quad + \theta\sigma_2) + \epsilon\theta\sigma_3) + (\epsilon\eta\theta + k_5(\alpha k_4 + \theta\gamma))\sigma_4) + K\beta\tau \\ &\quad (k_7(k_5(k_4 + \theta\phi_1) + \epsilon\theta\phi_2) + (\epsilon\eta\theta + k_5(\alpha k_4 + \theta\gamma))\phi_3))). \end{aligned} \tag{3.8}$$

The threshold parameter $\mathcal{R}_C$ displays the contribution of the human population, denoted by $\mathcal{R}_H$, and the contribution by the bacteria concentration in the environment, denoted by $\mathcal{R}_E$. So that

$$\mathcal{R}_C = \mathcal{R}_H + \mathcal{R}_E,$$

where,

$$\begin{aligned} \mathcal{R}_H &= \frac{\beta}{k_1k_3k_4k_5k_7}(\omega k_3(\epsilon(k_7\phi_2 + \eta\phi_3) + k_5(k_7\phi_1 + \gamma\phi_3)) \\ &\quad + k_2(k_4k_5(k_7 + \alpha\phi_3) + \epsilon\theta(k_7\phi_2 + \eta\phi_3) + \theta k_5(k_7\phi_1 + \gamma\phi_3)), \end{aligned} \tag{3.9}$$

$$\begin{aligned} \mathcal{R}_E &= \frac{\nu\pi}{K\tau k_1k_3k_4k_5k_7\mu}(\omega k_3(k_7(k_5\sigma_2 + \epsilon\sigma_3) + (\epsilon\eta + k_5\gamma)\sigma_4) \\ &\quad + k_2(k_7(k_5(k_4\sigma_1 + \theta\sigma_2) + \epsilon\theta\sigma_3) + (\epsilon\eta\theta + k_5(\alpha k_4 + \theta\gamma))\sigma_4)). \end{aligned} \tag{3.10}$$

Further, $\mathcal{R}_H$ encompasses the infectious contribution of individuals with gastric ulcers, the screened individuals, individuals undergoing treatment, and individuals with gastric cancer, respectively denoted by $\mathcal{R}_H^I, \mathcal{R}_H^{I_S}, \mathcal{R}_H^T$, and $\mathcal{R}_H^{I_C}$. Thus,

$$\begin{aligned}
\mathcal{R}_H^I &= \frac{\beta k_2}{k_1 k_3}, \\
\mathcal{R}_H^{I_S} &= \frac{\beta\phi_1(\theta k_2 + \omega k_3)}{k_1 k_3 k_4}, \\
\mathcal{R}_H^T &= \frac{\beta\phi_2\epsilon(\theta k_2 + \omega k_3)}{k_1 k_3 k_4 k_5}, \\
\mathcal{R}_H^{I_C} &= \frac{\beta\phi_3\left[\omega k_3(\epsilon\eta + k_5\gamma) + k_2(\epsilon\eta\theta + \alpha k_4 k_5 + \theta k_5\gamma)\right]}{k_1 k_3 k_4 k_5 k_7}.
\end{aligned}$$

3.3. Existence of endemic equilibrium

Theorem 3.3. *The Model* (2.10) *admits a unique endemic equilibrium (EE), whenever* $\mathcal{R}_H > 1$ *and* $\mathcal{R}_E > 1$.

Proof. Let $P^* = \left(S^*, E^*, I^*, I_S^*, T^*, I_C^*, B^*\right)$ denote any non-trivial solution of System (2.10). Then, solving the system at the steady state in terms of force of infection $\lambda := \lambda^*$ yields

$$\begin{cases}
S^* &= \dfrac{\pi + \zeta T^*}{\lambda^* + \mu}, \\
E^* &= \dfrac{\lambda^*(\pi + \zeta T^*)}{k_1(\lambda^* + \mu)}, \\
I^* &= \dfrac{\lambda^*(\pi + \zeta T^*)\rho}{k_1 k_3(\lambda^* + \mu)}, \\
I_S^* &= \dfrac{\lambda^*(\pi + \zeta T^*)(\theta\rho + \omega k_3)}{k_1 k_3 k_4(\lambda^* + \mu)}, \\
T^* &= \dfrac{\lambda^*(\pi + \zeta T^*)(\theta\rho + \omega k_3)\epsilon}{k_1 k_3 k_4(\lambda^* + \mu)}, \\
I_C^* &= \dfrac{\lambda^*(\pi + \zeta T^*)\beta\left[\omega k_3(\epsilon\eta + k_5\gamma) + \rho(\epsilon\eta\theta + \alpha k_4 k_5 + \theta k_5\gamma)\right]}{k_1 k_3 k_4 k_5 k_7(\lambda^* + \mu)}, \\
B^* &= \dfrac{\lambda^*(\pi + \zeta T^*)}{k_1 k_3 k_4 k_5 k_7\tau(\lambda^* + \mu)}\left[\omega k_3\left(k_7(k_5\sigma_2 + \epsilon\sigma_3) + (\epsilon\eta + k_5\gamma)\sigma_4\right)\right. \\
&\quad \left. + \rho\left(k_7(k_5(k_4\sigma_1 + \theta\sigma_2) + \epsilon\theta\sigma_3) + (\epsilon\eta\theta + k_5(\alpha k_4 + \theta\gamma))\sigma_4\right)\right].
\end{cases} \tag{3.11}$$

As it is established by (2.2), the force of infection with $\lambda := \lambda^*$ is given as

$$\lambda^* = \frac{\beta\left(I^* + I_S^*\phi_1 + T^*\phi_2 + I_C^*\phi_3\right)}{N^*} + \frac{\nu B^*}{K + B^*}. \tag{3.12}$$

From Model (2.10), $N^* = S^* + E^* + I^* + I_S^* + T^* + I_C^*$. Thus, adding the first six equations of system (3.11) gives N^* as,

$$N^* = \left(\frac{\pi + \zeta T^*}{\lambda^* + \mu}\right)\left[1 + \lambda^*\Big(\rho(k_4 k_5(\alpha + k_7) + \epsilon\theta(\eta + k_7) + \theta k_5(\gamma + k_7)\right)$$

$$+k_3(\epsilon\omega(\eta+k_7)+k_5(\omega\gamma+(\omega+k_4)k_7))\Big)\Big]. \tag{3.13}$$

For convenience in (3.13), let

$$\begin{aligned}\Delta_0 &= (\rho(k_4k_5(\alpha+k_7)+\epsilon\theta(\eta+k_7)+\theta k_5(\gamma+k_7))+k_3(\epsilon\omega(\eta+k_7)\\ &\quad +k_5(\omega\gamma+(\omega+k_4)k_7)).\end{aligned} \tag{3.14}$$

So that it becomes

$$N^* = \left(\frac{\pi+\zeta T^*}{\lambda^*+\mu}\right)\Big[1+\lambda^*\Delta_0\Big]. \tag{3.15}$$

Solving the first part of the right-hand side of (3.12) and writing it in terms of $\mathcal{R}_H$, we obtain

$$\lambda_H^* = \frac{\lambda^*(\pi+\zeta T^*)\mathcal{R}_H}{(\lambda^*+\mu)N^*} \tag{3.16}$$

Inserting (3.15) in (3.16), we get

$$\lambda_H^* = \frac{\lambda^*\mathcal{R}_H}{1+\Delta_0\lambda^*}. \tag{3.17}$$

Solving the second part of the right-hand side of (3.12) and writing it in terms of $\mathcal{R}_E$ gives

$$\lambda_E^* = \frac{\nu B^*}{K+B^*} = \frac{\nu B^*}{K}\left[\frac{1}{1+\frac{B^*}{K}}\right] = \frac{\nu\mu\lambda^*(\pi+\zeta T^*)\mathcal{R}_E}{(\lambda^*+\mu)\nu\pi+\lambda^*\mu(\pi+\zeta T^*)\mathcal{R}_E}. \tag{3.18}$$

Thus, combining (3.17) and (3.18) yields

$$\lambda^* = \frac{\mathcal{R}_H\lambda^*}{1+\Delta_0\lambda^*}+\frac{\nu\mu\lambda^*(\pi+\zeta T^*)\mathcal{R}_E}{(\lambda^*+\mu)\nu\pi+\lambda^*\mu(\pi+\zeta T^*)\mathcal{R}_E}. \tag{3.19}$$

Rearranging (3.19), we obtain a quadratic equation of the form

$$b_0\lambda^{*2}+b_1\lambda^*+b_2=0, \tag{3.20}$$

where the values of coefficient are given as follows,

$$\begin{cases} b_0 = \Delta_0\nu\frac{\pi}{\mu}+\Delta_0(\pi+\zeta T^*)\mathcal{R}_E,\\ b_1 = (\pi+\zeta T^*)\mathcal{R}_E(1-\mathcal{R}_H)+\nu\frac{\pi}{\mu}(1-\mathcal{R}_H)+\pi\nu\Delta_0(1-\mathcal{R}_H)-\Delta_0\nu\zeta T^*\mathcal{R}_E,\\ b_2 = \nu\pi(1-\mathcal{R}_H)-\nu(\pi+\zeta T^*)\mathcal{R}_E. \end{cases} \tag{3.21}$$

So, the solution of the Eq. (3.20) is given as

$$\lambda^* = \frac{-b_1\pm\sqrt{b_1^2-4b_0b_2}}{2b_0}. \tag{3.22}$$

From Eq. (3.22), we claim that, Model (2.10) has:

Case 1: A unique endemic equilibrium if $b_1^2 - 4b_0b_2 = 0$.

Case 2: Two endemic equilibria if $b_2 < 0$ and $b_1^2 - 4b_0b_2 > 0$.

Case 3: No endemic equilibrium otherwise.

We note that a positive endemic equilibrium exists when the reproduction number is greater than unity [22] and thus in Model (2.10), an interior endemic equilibrium exists whenever $\mathcal{R}_H > 1$ and $\mathcal{R}_E > 1$. In case 1, it is clear that if $b_1^2 - 4b_0b_2 = 0$ then we will have a unique endemic equilibrium which is negative, and in case 3, no endemic equilibrium point exists at all. Therefore, only **Case 2** guarantees the existence of at least one positive endemic equilibrium. Since it is biologically sound that the endemic equilibrium must be positive, then based on Case 2, we further give narrower conditions for the existence of at least one positive endemic equilibrium as follows:

(i) One unique positive endemic equilibrium if $b_1 < 0$ and $b_1 < \sqrt{b_1^2 - 4b_0b_2}$ or $b_1 > 0$ and $b_1 < \sqrt{b_1^2 - 4b_0b_2}$.

(ii) Two positive endemic equilibria if $b_1 < 0$ and $b_1 > \sqrt{b_1^2 - 4b_0b_2}$.

(iii) No positive endemic equilibrium otherwise.

Holding **Case 2** true, we use Descartes' rule of sign changes to examine the signs of the coefficients of Equation (3.20). Thus, it is clear from Equation (3.21) that $b_0 > 0$ and $b_2 < 0$ if and only if $\mathcal{R}_H > 1$ and $\mathcal{R}_E > 1$. However, the sign of b_1 is not clear. Thus, we summarize the condition for the existence of at least one positive EE in Table 1 as follows:

Table 1. Existence of positive endemic equilibrium of the system (2.10).

Sign of b_0	sign of b_1	sign of b_2	number of sign changes	Conclusion
+	-	-	1	a unique endemic equilibrium
+	+	-	1	a unique endemic equilibrium

Hence, based on the results in Table 1, it is clear that the Model (2.10) has a unique endemic equilibrium whenever $\mathcal{R}_H > 1$ and $\mathcal{R}_E > 1$. This completes the proof. □

3.4. Stability analysis

Theorem 3.4. *The disease-free equilibrium of Model* (2.10) *is locally asymptotically stable (LAS) whenever* $\mathcal{R}_C < 1$ *and unstable if* $\mathcal{R}_C > 1$. *In the latter case, Model* (2.10) *has a unique endemic equilibrium which is LAS for* $\mathcal{R}_C$ *close to 1.*

Proof. The first part of the Theorem follows from [23]. We prove the second part of the Theorem using the Center Manifold Theory presented in [24]. Since the disease-free equilibrium changes its stability at $\mathcal{R}_C = 1$, we choose $\mathcal{R}_C = 1$ as the bifurcation parameter. Let β^* and ν^* be respectively the critical values of β and ν at $\mathcal{R}_C = 1$ such that β^* and ν^* are given by

$$\beta^* = \frac{k_1k_3k_4k_5k_7}{Q} \quad \text{and} \quad \nu^* = \frac{K\tau k_1k_3k_4k_5k_7}{\mathcal{G}},$$

where,

$$\begin{aligned} Q &= \omega k_3(\epsilon(k_7\phi_2+\eta\phi_3)+k_5(k_7\phi_1+\gamma\phi_3))+k_2(k_4k_5(k_7+\alpha\phi_3)+\epsilon\theta(k_7\phi_2+\eta\phi_3)\\ &\quad +\theta k_5(k_7\phi_1+\gamma\phi_3),\\ \mathcal{G} &= \frac{\pi}{\mu}(\omega k_3(k_7(k_5\sigma_2+\epsilon\sigma_3)+(\epsilon\eta+k_5\gamma)\sigma_4)+k_2(k_7(k_5(k_4\sigma_1+\theta\sigma_2)+\epsilon\theta\sigma_3)\\ &\quad +(\epsilon\eta\theta+k_5(\alpha k_4+\theta\gamma))\sigma_4)). \end{aligned}$$

The Jacobian matrix J ($\mathcal{E}^0$) at the DFE when $\beta=\beta^*$ and $\nu=\nu^*$ is given as

$$J(\mathcal{E}^0)=\begin{pmatrix} -\mu & 0 & -\beta^* & -\beta^*\phi_1 & \zeta-\beta^*\phi_2 & -\beta^*\phi_3 & \frac{-\nu^*\pi}{K\mu}\\ 0 & -k_1 & \beta^* & \beta^*\phi_1 & \beta^*\phi_2 & \beta^*\phi_3 & \frac{\nu^*\pi}{K\mu}\\ 0 & k_2 & -k_3 & 0 & 0 & 0 & 0\\ 0 & \omega & \theta & -k_4 & 0 & 0 & 0\\ 0 & 0 & 0 & \epsilon & k_5 & 0 & 0\\ 0 & 0 & \alpha & \gamma & \eta & -k_7 & 0\\ 0 & 0 & \sigma_1 & \sigma_2 & \sigma_3 & \sigma_4 & -\tau \end{pmatrix}.$$

So that the right eigenvector $W=(w_1,w_2,w_3,w_4,w_5,w_6,w_7)^T$ associated with zero eigenvalue is given as

$$\begin{cases} w_1 &= \frac{-\beta^*(\omega_3+\phi_1w_4+\phi_2w_5+\phi_3w_6)-\frac{\nu^*\pi}{K\mu}}{\mu},\\ w_2 &= w_2>0,\\ w_3 &= \frac{k_2w_2}{k_3},\\ w_4 &= \frac{\omega w_2+\theta w_3}{k_4},\\ w_5 &= \frac{\epsilon w_4}{k_5},\\ w_6 &= \frac{\alpha w_3+\gamma w_4+\eta w_5}{k_7},\\ w_7 &= \frac{\sigma_1w_3+\sigma_2w_4+\sigma_3w_5+\sigma_4w_6}{\tau}. \end{cases} \tag{3.23}$$

Similarly, the left eigenvector $V=(v_1,v_2,v_3,v_4,v_5,v_6,v_7)^T$ associated with zero eigenvalue is given as

$$\begin{cases} v_1 &= 0,\\ v_2 &= \frac{k_2v_3}{\omega v_4},\\ v_3 &= \frac{\beta^*v_2+\theta v_4+\alpha v_6+\phi_1v_7}{k_3},\\ v_4 &= \frac{\epsilon v_5+\gamma v_6+\sigma_2v_7+\beta^*\phi_1v_2}{k_4},\\ v_5 &= \frac{\epsilon w_4}{k_5},\\ v_6 &= \frac{\epsilon v_6+\sigma_3+\beta^*\phi_2v_2}{k_7},\\ v_7 &= \frac{\nu^*\pi v_2}{\tau K\mu}. \end{cases} \tag{3.24}$$

As per the Theory, we compute the coefficients a and b defined by

$$a = \sum_{k,i,j=1}^{n} v_k w_i w_j \frac{\partial^2 f_k}{\partial x_i \partial x_j}\left(\mathcal{E}^0, \beta^*\right), \quad b = \sum_{k,i=1}^{n} v_k w_i \frac{\partial^2 f_k}{\partial x_i \partial \beta}\left(\mathcal{E}^0, \beta^*\right). \tag{3.25}$$

Thus, we obtain,

$$a = 2v_2\left(w_1 w_2 \frac{\beta^*\mu}{\pi} + w_1 w_4 \frac{\beta^*\mu\phi_1}{\pi} + w_1 w_5 \frac{\beta^*\mu\phi_2}{\pi} + w_1 w_6 \frac{\beta^*\phi_3\mu}{\pi} + w_1 w_7 \frac{\nu^*}{K}\right) < 0, \tag{3.26}$$

$$b = v_2\left(w_2 + w_4\phi_1 + w_5\phi_2 + w_6\phi_3 + w_7 \frac{\pi}{\mu K}\right) > 0. \tag{3.27}$$

Since $a < 0$ and $b > 0$, they clearly differ in sign. Thus, Model (2.10) undergoes a forward (transcritical) bifurcation at $\mathcal{R}_C = 1$. Thus, the endemic equilibrium is LAS for $\mathcal{R}_C > 1$. □

Theorem 3.5. *The disease-free equilibrium of Model* (2.10) *is globally asymptotically stable (GAS) whenever* $\mathcal{R}_H < 1$.

Proof. Let's consider the candidate Lyapunov function [25] of the form

$$L(E, I, I_S, T, I_C) = E + p_0 I + p_1 I_S + p_2 T + p_3 I_C, \tag{3.28}$$

where p_0, p_1, p_2 and p_3 are positive constant to be determined. Since $\frac{S}{N} \leq 1$, then the time derivative of L along the trajectories of model (2.10) is such that

$$\begin{aligned}
\frac{dL}{dt} &\leq \beta\left(I + \phi_1 I_s + \phi_2 T + \phi_3 I_c\right) - k_1 E + p_0\left(k_2 E - k_3 I\right) + p_1\left(\omega E + \theta I - k_4 I_s\right) \\
&\quad + p_2\left(\epsilon I_s - k_5 T\right) + p_3\left(\alpha I + \gamma I_s + \eta T - k_7 I_c\right), \\
&= \left(-k_1 + k_2 p_0 + \omega p_1\right) E + \left(\beta - k_3 p_0 + \theta p_1 + \alpha p_3\right) I + \left(\beta\phi_1 - k_4 p_1 + \epsilon p_2 + \gamma p_3\right) I_S \\
&\quad + \left(\beta\phi_2 + \eta p_3 - k_5 p_2\right) T + \left(\beta\phi_3 - k_7 p_3\right) I_C.
\end{aligned} \tag{3.29}$$

We choose p_0, p_1, p_2 and p_3 such that

$$\begin{cases}
-k_1 + k_2 p_0 + \omega p_1 = 0, \\
\beta - k_3 p_0 + \theta p_1 + \alpha p_3 = 0, \\
\beta\phi_1 - k_4 p_1 + \epsilon p_2 + \gamma p_3 = 0, \\
\beta\phi_2 + \eta p_3 - k_5 p_2 = 0, \\
\beta\phi_3 - k_7 p_3 = 0.
\end{cases} \tag{3.30}$$

Solving the system (3.30) we obtain

$$\begin{cases}
p_0 = \dfrac{1}{k_3 k_4 k_5 k_7}\beta\left[k_4 k_5(k_7 + \alpha\phi_3) + \epsilon\theta(k_7\phi_2 + \eta\phi_3) + \theta k_5(k_7\phi_1 + \gamma\phi_3)\right], \\
p_1 = \dfrac{1}{k_4 k_5 k_7}\beta\left[\epsilon(k_7\phi_2 + \eta\phi_3) + k_5(k_7\phi_1 + \gamma\phi_3)\right], \\
p_2 = \dfrac{\beta k_7\phi_2 + \beta\eta\phi_3}{k_5 k_7}, \\
p_3 = \dfrac{\beta\phi_3}{k_7}.
\end{cases} \tag{3.31}$$

Substituting (3.31) in (3.29) we have

$$\frac{dL}{dt} \leq (\mathcal{R}_H - 1)k_1 E.$$

Clearly, $\frac{dL}{dt} < 0$ if $\mathcal{R}_H < 1$ or $\frac{dL}{dt} = 0$ if $E = 0$. Thus, L is a strict Lyapunov function for the Model (2.10) and thus, the DFE is GAS. Hence, proved. □

Theorem 3.6. *The endemic equilibrium of Model* (2.10) *is globally asymptotically stable whenever* $\mathcal{R}_H > 1$.

The proof of the theorem (3.6) is presented later in Appendix A.

4. Numerical analysis

We use the parameter values given in Table 2 to perform the sensitivity analysis and simulations of the model. Most of the parameter values are obtained from the existing literature, while a few are assumed.

4.1. Sensitivity analysis

Sensitivity analysis is a crucial tool in mathematical modeling, especially in epidemiology. It entails evaluating how changes in parameters in the model affect the reproduction number of the model. This analysis aids in determining which model parameters have the most influence on disease transmission and can guide the development of efficient control measures. In this research, we focus on these parameters of interest, which are ω, the screening rate of the exposed population, θ, the screening rate of the infected population with gastric ulcers, and ϵ, the treatment rate of the screened population. This is done graphically using equation (3.8) for the control reproduction number against the parameters of interest. The results obtained are depicted by Figure 2 and 3.

Figure 2(a) shows the influence of screening of the exposed population on the control reproduction number. From the graph, we observe that an increase in screening of exposed individuals leads to a decrease in the control reproduction number, $\mathcal{R}_C$, and vice versa. This is because early detection of the infection via screening gives time for treatment, which helps in lowering the rate of transmission. The observation outlines that $\mathcal{R}_C$ is very sensitive to changes in ω. Therefore, enhancing efforts in screening, especially among exposed individuals, should be prioritized as a measure to effectively reduce infection transmission. Figure 2(b) shows the effectiveness of treatment for screened individuals with gastric ulcers on the control reproduction number. The graph shows that the treatment rate of screened individuals increases as the control reproduction number decreases. This means that increasing the effectiveness of treatment will lower the reproduction number, making it a significant parameter to control gastric ulcers and their progression to gastric cancer.

Figure 2(c) represents the screening of gastric ulcers on the $\mathcal{R}_C$. The graph indicates a sharp decline in $\mathcal{R}_C$ as θ increases, especially at the initial values of θ. After a certain point, when ($\theta > 0.2$), the curve begins to flatten, indicating that even at a slower rate of screening, the infection can be reduced significantly. Comparing Figure 2(a) and 2(c), ω has a significant role in $\mathcal{R}_C$ than θ. From this, we can deduce that early screening is ideal compared to late screening. This suggests that screening

Table 2. Parameter description of dynamic system (2.10). We once more note that, as per the assumptions **A4** and **A5**, $\gamma = \alpha$ and $\sigma_2 = \sigma_1$ respectively.

Parameter	Description	Value per year	Source
π	Recruitment rate of susceptible population.	200,000	[26]
μ	Natural death rate.	0.000019	[12]
τ	Natural death rate of *H. pylori* bacteria.	0.00167	[12]
δ	Death rate due to gastric cancer.	0.00839	[10]
ζ	Recovery rate of treated humans with gastric ulcers.	0.00116	[27]
β	Effective contact rate of susceptible individuals with *H. pylori* bacteria.	2.0414	Assumed
ω	Screening rate from Exposed individuals.	0.496	[28]
ϵ	The rate at which the screened population gets treatment.	0.5093	[29]
η	Rate at which treated individuals develop gastric cancer due to drug resistance, non-adherence to drugs prescription, etc.	0.0017	[11]
θ	Screening rate for infected individuals with gastric ulcers.	0.224	[28]
σ_1	*H. pylori* shedding rate by gastric ulcers.	0.0008	[10]
σ_2	*H. pylori* shedding rate by the screened individuals.	0.0008	Assumed
σ_3	Shedding rate of individuals undergoing treatment.	0.0004	[10]
σ_4	Shedding rate of gastric cancer individuals.	0.0001	[10]
ρ	Rate at which exposed individuals joins gastric ulcers infected humans.	0.603	[27]
α	Rate at which infected individuals with gastric ulcers develop gastric cancer.	0.438	[30]
γ	Rate at which screened individuals develop gastric cancer.	0.438	Assumed
K	Concentration of *H. pylori* in foods or water.	50,000	[31]
ν	Ingestion rate of *H. pylori* bacteria.	0.7	[10]
ϕ_1	Transmission coefficient for screened infectious individuals.	0.003	Assumed
ϕ_2	Transmission coefficient for screened individuals undergoing treatment.	0.002	Assumed
ϕ_3	Transmission coefficient for infectious gastric cancer individuals.	0.001	Assumed

of exposed individuals shapes the gastric cancer problem; if more individuals are screened, then the burden of gastric cancer can be controlled well.

Figure 2(d) shows the variation of control reproduction number with effective contact rate at increasing values of ω. We observe that, when the screening rate for exposed individuals increases, the control reproduction number decreases, consequently reducing the rate of transmission of infections. Screening and treating infected individuals help to reduce reactivation and, consequently, decrease the overall transmission of the infection within the population. Individuals who are infected but do not exhibit symptoms frequently carry on with their normal activities without seeking medical attention. They consequently unknowingly come into contact with vulnerable individuals, which increases the risk of disease transmission. Therefore, it is crucial to screen all individuals as they can continuously

spread the infection without being aware of it.

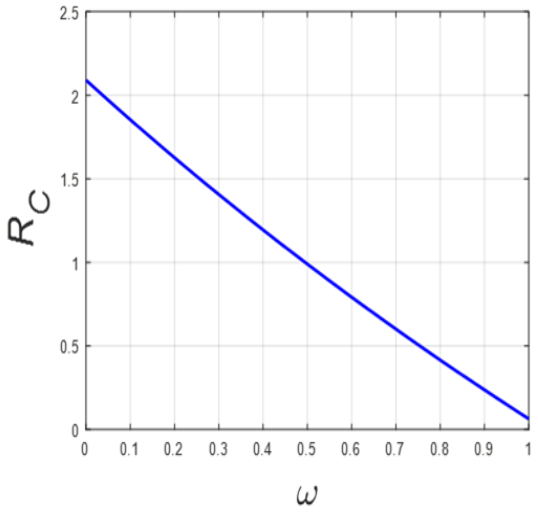

(a) Impact of ω (screening of asymptomatic individuals) on the control reproduction number.

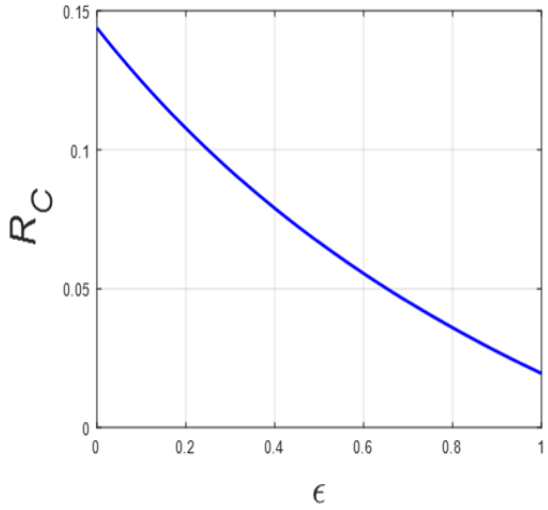

(b) Impact of ϵ (rate of treatment on screened individuals with gastric ulcers) on the control reproduction number.

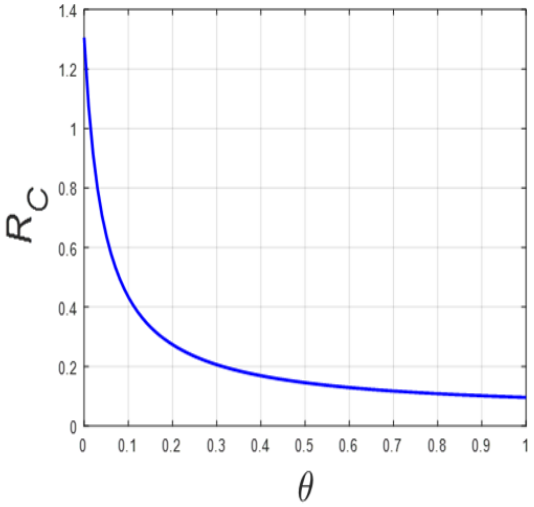

(c) Impact of θ (rate of screening for gastric ulcer individuals) on the control reproduction number.

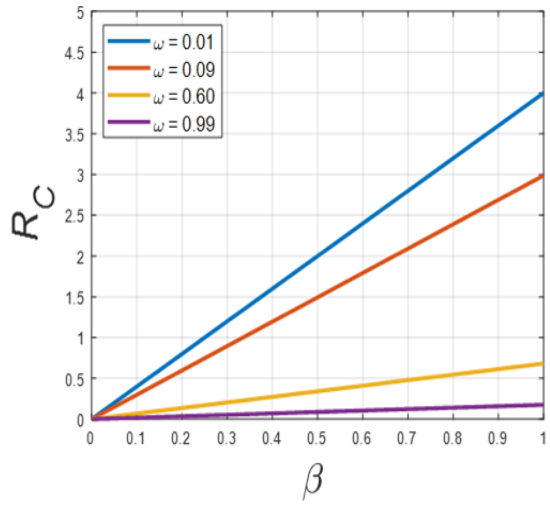

(d) Variation of $\mathcal{R}_C$ with β (effective contact rate) at increasing values of ω (screening of exposed individuals).

Figure 2. Variation of control reproduction number, $\mathcal{R}_C$ with ω, ϵ, θ and β.

Figure 3(a) is the surface plot showing how $\mathcal{R}_C$ varies with respect to ω and ϵ. We observe from the figure that, as ω and ϵ decrease, the $\mathcal{R}_C$ increases. This indicates that an increase in screening rate, ω, and treatment rate ϵ, results in a decrease in the $\mathcal{R}_C$, showing that the combination of both measures contributes significantly to controlling the spread of the infection. Figure 3(c) is a contour plot visualization of Figure 3(a). Figure 3(b) represents the surface plot for the variation of $\mathcal{R}_C$ with respect to ϵ and θ. The findings from this figure are comparable to what is observed in Figures 2(b)

and 2(c) jointly. Figure 3(d) is a contour plot visualization of Figure 3(b).

4.2. Simulations

Many individuals in rural areas may develop gastric ulcers and become ignorant of their status. Screening of infected individuals can help individuals to know their status of gastric ulcers earlier. Figures 4(a) and 4(b) reveal that the number of screened humans increases proportionally with the rate of screening of exposed and infected individuals with gastric ulcers, respectively. This is because, as the screening rate increases, more humans will know their status and move to the screened compartment, leading to the replenishment of the class. Thus, an increase in screening rate significantly boosts early detection, prevents transmission of infections and other complications such as gastric cancer.

From Figures 5(a) and 5(b), gastric cancer can be controlled by screening infectious individuals. Screening and treating will decrease the number of *H. pylori* bacteria in the environment since infectious individuals are responsible for shedding *H. pylori* in the environment.

Individuals in the gastric ulcers class and *H. pylori* bacteria in the environment decreases when the rates of screening increases. From Figure 6(a), it can be seen that the number of individuals with gastric ulcers decreases with time due to effective screening of exposed humans. Increasing the screening rate for exposed humans assists in lowering the number of infected individuals with gastric ulcers and also suppresses the growth of the bacteria population over a given time, as indicated in Figure 6(b).

The simulations show that being aware of the status of gastric ulcers in the absence of treatment, although informative, does not directly aid in controlling the disease. Intervention methods such as early screening, treatment, and prevention efforts are very critical to effective control. Thus, this subsection explores the gastric ulcers' dynamics when screened individuals are treated and the impact of treatment on the gastric cancer individual. Individuals who are identified through screening for gastric ulcers are certain to obtain appropriate medical attention and achieve better health results when they receive effective treatment. Thus, leave the screened infected class decreasing the overall number in that class as demonstrated in Figure 7(a). This indicates that fewer individuals remain in the screened compartment as the treatment becomes more effective. As the treatment rate increases, the number of screened individuals decreases, which results in a decrease in the number of gastric cancer cases, as shown in Figure 7(b). This indicates that incorporating screening and effective treatment significantly slows down the development of gastric ulcers to gastric cancer, underscoring the vital role of early control measures in disease management.

From Figure 8(a), the number of infected humans with gastric ulcers decreases significantly as the effectiveness of screening and treatment increases. For example, at ($\omega = \epsilon = 0.1$), the number of gastric ulcer cases reaches $230,000$, at equilibrium, while at ($\omega = \epsilon = 0.7$), the number of individuals with gastric ulcer levels off to $50,000$. Thus, higher effectiveness of screening and treatment lowers the number of infected cases significantly. This indicates that early detection and effective treatment can control the spread of gastric ulcers and their impacts on gastric cancer.

From Figure 8(b), it is evident that both screening and treatment play a vital role in increasing the number of individuals who enter and remain in the screening class. The number of screened individuals increases with time as the effectiveness of screening and treatment increases. The curve tends to flatten after 20 to 35 years, showing that the screened individuals reach equilibrium. This implies that effective screening enhances the early detection of gastric ulcers, whereas effective treatment ensures that the individuals who have been identified are managed properly, thus preventing reinfection and loss from

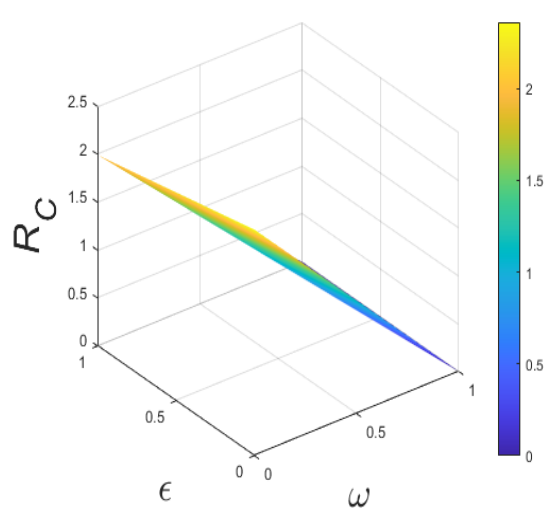

(a) Impact of ϵ (treatment rate of screened humans) and ω (screening rate of Exposed humans) on the control reproduction number.

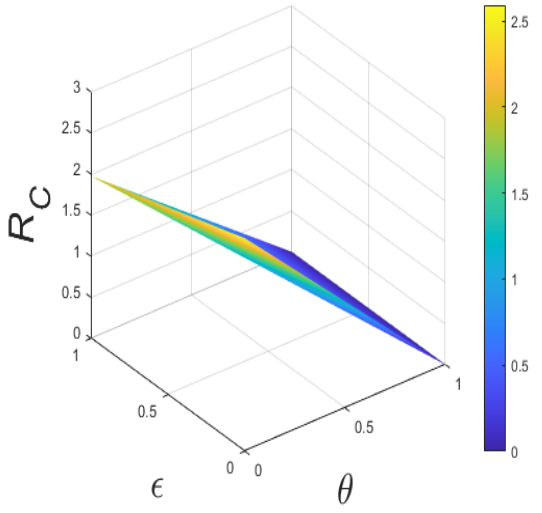

(b) Impact of ϵ (treatment rate of screened humans) and θ (screening rate of humans with gastric ulcers) on the control reproduction number.

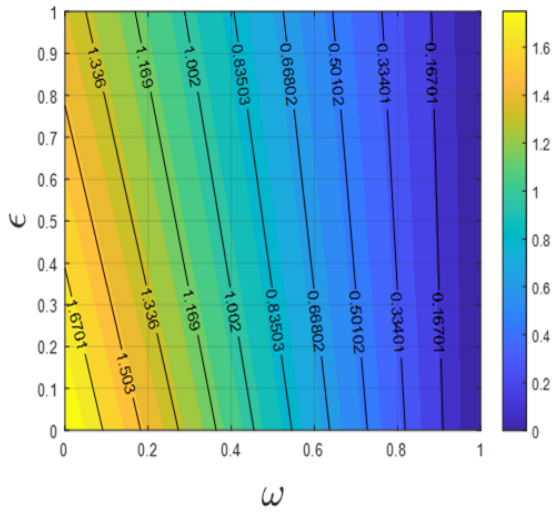

(c) Contour plot visualization for Figure 3(a).

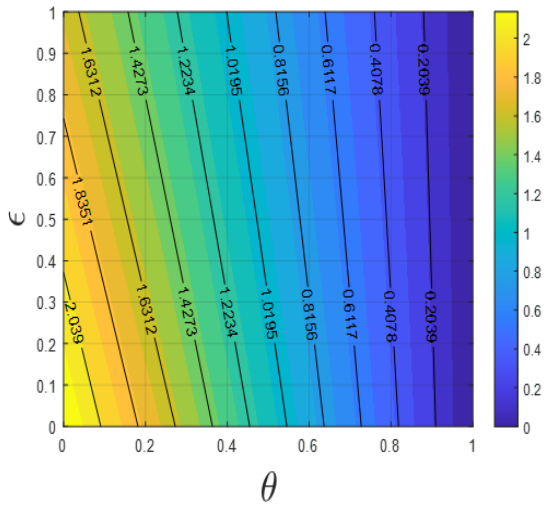

(d) Contour plot visualization for Figure 3(b).

Figure 3. Variation of the control reproduction number, $\mathcal{R}_C$ with respect to ω, θ and ϵ.

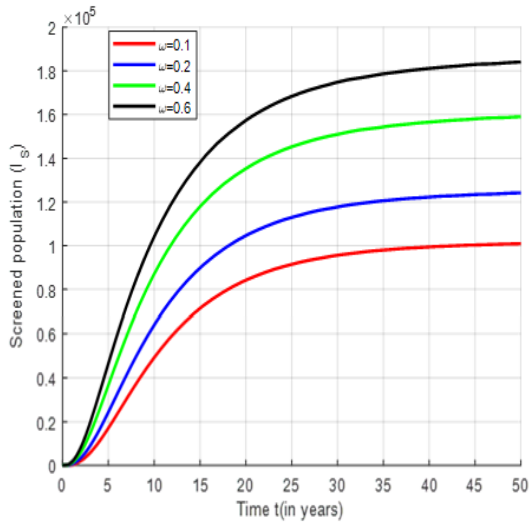

(a) Impact of ω (screening rate for exposed humans) on screened population.

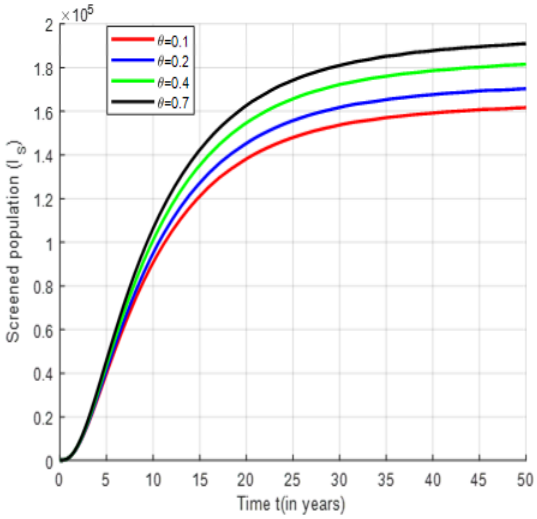

(b) Impact of θ (screening rate for infected humans with gastric ulcers) on screened population.

Figure 4. Impact of ω and θ on screened population.

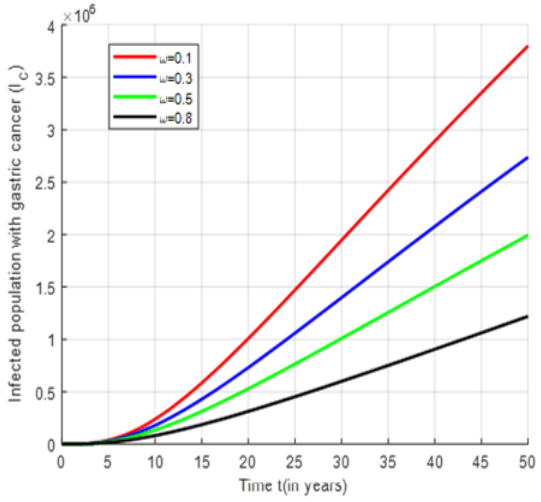

(a) Impact of ω (screening rate for exposed humans) on infected individuals with gastric cancer.

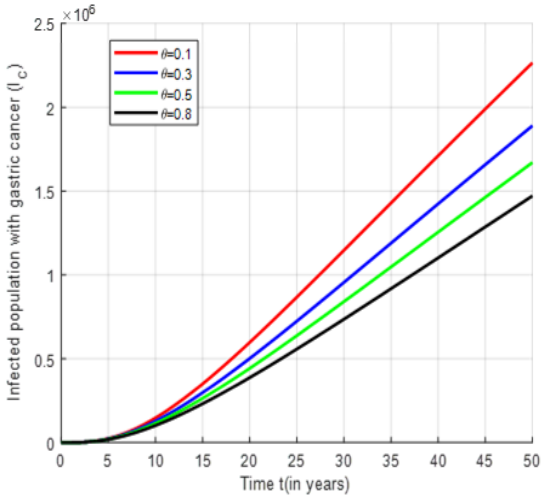

(b) Impact of θ (screening rate for infected humans with gastric ulcers) on infected humans with gastric cancer.

Figure 5. Impact of ω and θ on gastric cancer (I_C) population.

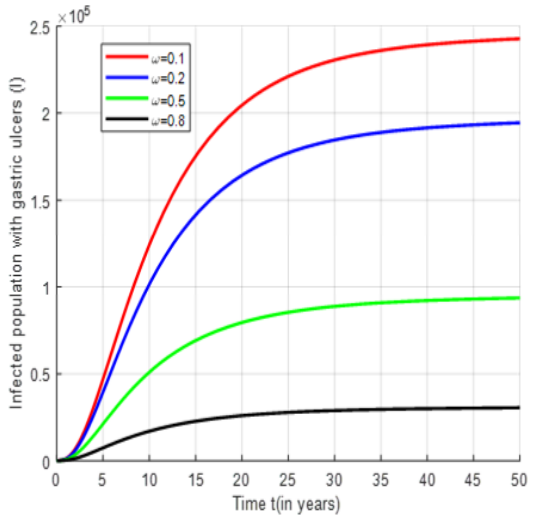

(a) Impact of ω (rate of screening for exposed humans) on gastric ulcers humans.

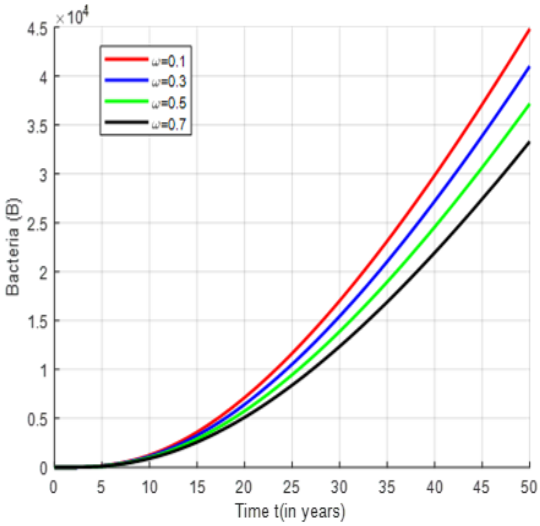

(b) Impact of ω (screening rate for exposed humans) on Bacteria population.

Figure 6. Impact of ω on infected individuals with gastric ulcers and Bacteria population.

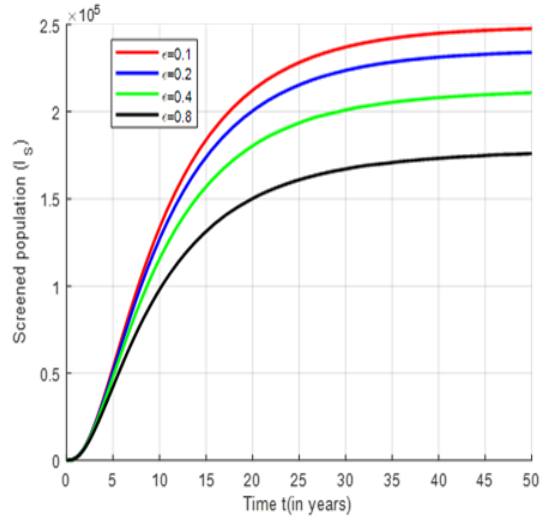

(a) Impact of ϵ (treatment rate of screened individuals) on Screened population.

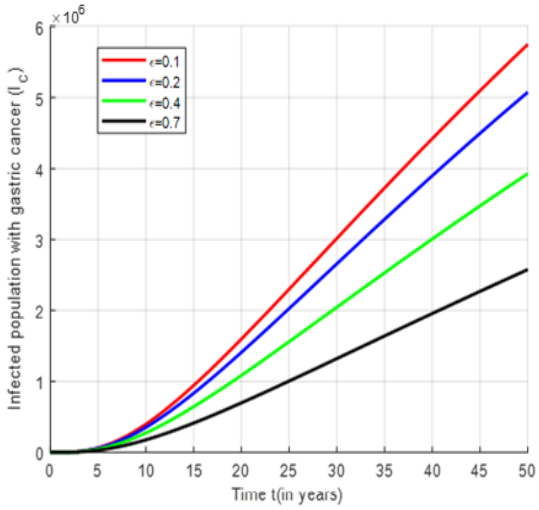

(b) Impact of ϵ (treatment rate of screened humans) on Infected population with gastric cancer.

Figure 7. Impact of ϵ on screened and Infected population with gastric cancer.

the screened class. The two control measures are crucial in increasing the participation of programs of screening, which will lead to early detection, management, and reduction of progression to gastric cancer.

Concurrent implementation of screening and treatment has more effects on transmission dynamics. As the effective screening and treatment are implemented, the individuals with gastric ulcers and the *H. pylori* bacteria concentration in the environment decreases. This reveals that screening and treatment of infectious individuals can help to lower the number of gastric ulcers, hence controlling the gastric cancer as seen in Figure 8(c). Figure 8(d) exhibits that in the presence of ineffective screening and treatment, the number of *H. pylori* bacteria rise rapidly as a result of the continued shedding rate of bacteria by infected individuals. It also indicates that when the screening and treatment are effective, that is, at ($\omega = \epsilon = 0.8$), the number of bacteria decreases.

5. Conclusions

In this work, we have formulated a compartmental mathematical model addressing the dynamics of gastric ulcers to gastric cancer. Key features that are incorporated in the model include the screening and treatment of gastric ulcers as a control strategy against gastric cancer. The model is thoroughly analyzed both quantitatively, qualitatively, and numerically. The main analytical and numerical results obtained indicate that;

- The model possesses a unique disease-free equilibrium which is locally and globally asymptotically stable when $\mathcal{R}_C < 1$.
- The model admits a unique endemic equilibrium which is locally and globally asymptotically stable whenever $\mathcal{R}_C > 1$.
- Screening alone for gastric ulcers is not an effective control measure, especially if treatment is not highly effective. As a result, the best control strategy should emphasize early screening rather than late screening in conjunction with efficient treatment.
- Early and late screening are essential for reducing transmission. Therefore, promoting screening at all levels can reduce $\mathcal{R}_C$ below unity and prevent the spread of gastric ulcer-related infections, especially gastric cancer.
- Further analysis has shown that effective screening and treatment play a vital role in the control of gastric ulcer transmission and, consequently, gastric cancer.

Therefore, based on the results, the study recommends the following:

- Serious sensitization and public awareness should be continuously conducted across the country to inform the general public on the benefits of early screening against gastric ulcers and gastric cancer, as well as encourage them to avail themselves of such screening. This should be done via organized campaigns, media such as TV, Radio, etc.
- Adequate screening facilities should be established in as many public health centers as possible to ensure early screening against gastric ulcers and gastric cancer for all individuals at risk. The facilities should be fully equipped.
- Health facilities should adopt electronic health records to ensure continuous, accurate, and available data to curb the problem of data limitations, especially for research purposes.

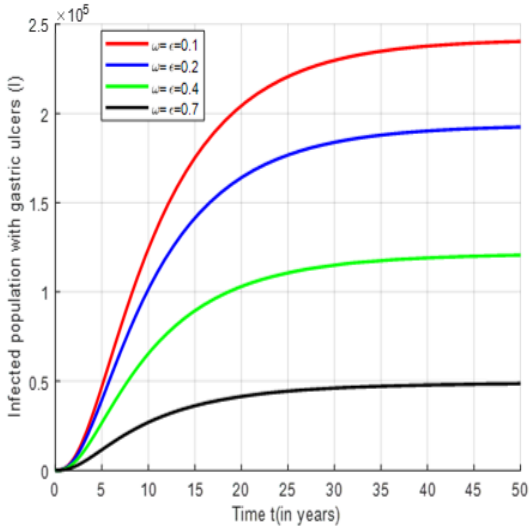

(a) Impact of ω (screening) and ϵ (treatment) on Infected humans (I).

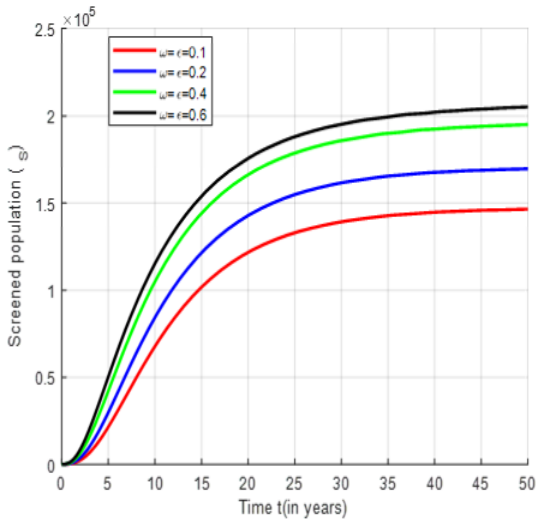

(b) Impact of ω (screening) and ϵ (treatment) on Screened humans (I_S).

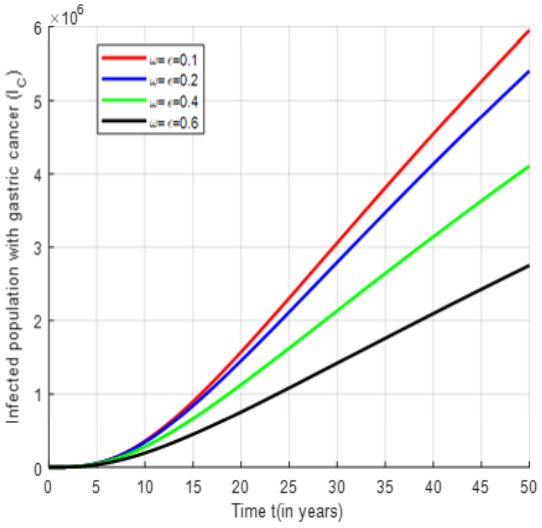

(c) Impact of ω (screening) and ϵ (treatment) on Infected humans (I_C) .

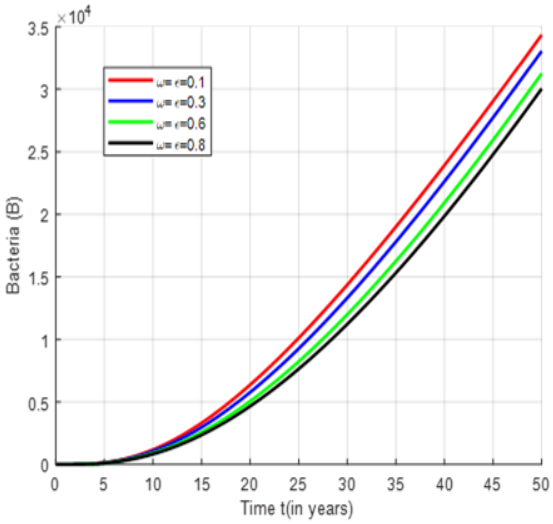

(d) Impact of ω (screening) and ϵ (treatment) on Bacteria concentration.

Figure 8. Impact of ω and ϵ on Infected (I), Screened (I_S), Infected (I_C) and Bacteria population.

- The government and public health officials should invest in diagnostic facilities and work more to train healthcare officials in electronic data handling.
- More community health-care promoters should be trained and strategically placed across the country for immediate response to public health issues.

These strategies not only assist in decreasing the spread of infections but also lower the risk of gastric ulcers progressing to gastric cancer. This underscores how vital it is to devote resources to enhancing diagnostic capacities and treatment efficacy. Therefore, in order to accomplish control sustainability, public health interventions should prioritize on creating awareness, early screening, and improving treatment.

Use of AI tools declaration

The authors declare they have not used Artificial Intelligence (AI) tools in the creation of this article.

Acknowledgments

GKM acknowledges the invaluable contribution from Mawazo Institute and its partners in supporting this research, which has been instrumental in making it successful. The authors are also thankful to the reviewers for their invaluable comments, which helped improve the quality of this study.

Conflict of interest

The authors declare there is no conflict of interest.

References

1. J. Ferlay, M. Colombet, I. Soerjomataram, D. M. Parkin, M. Pieros, A. Znaor, et al., Cancer statistics for the year 2020: An overview, *Int. J. Cancer*, **149** (2021), 778–789. https://doi.org/10.1002/ijc.33588
2. J. Ferlay, M. Colombet, I. Soerjomataram, C. Mathers, D. M. Parkin, M. Pieros, et al., Estimating the global cancer incidence and mortality in 2018: GLOBOCAN sources and methods, *Int. J. Cancer*, **144** (2019), 1941–1953. https://doi.org/10.1002/ijc.31937
3. V. E. Reyes, *Helicobacter pylori* and its role in gastric cancer, *Microorganisms*, **11** (2023), 1312. https://doi.org/10.3390/microorganisms11051312
4. M. Shen, R. Xia, Z. Luo, H. Zeng, W. Wei, G. Zhuang, et al., The long-term population impact of endoscopic screening programmes on disease burdens of gastric cancer in China: A mathematical modelling study, *J. Theor. Biol.*, **484** (2020), 109996. https://doi.org/10.1016/j.jtbi.2019.109996
5. E. A. V. Noguera, S. C. Trujillo, E. Ibargüen-Mondragón, A within-host model on the interactions of sensitive and resistant *Helicobacter pylori* to antibiotic therapy considering immune response, *Math. Biosci. Eng.*, **22** (2025), 185–224. https://doi.org/10.3934/mbe.2025009
6. V. R. RaviKKumar, S. Rathi, S. Singh, B. Patel, S. Singh, K. Chaturvedi, et al., A comprehensive review on Ulcer and their treatment, *Chinese J. Appl. Physiol.*, **39** (2023), e20230006. https://doi.org/10.62958/j.cjap.2023.006

7. A. H. Khan, M. A. Dar, M. A. Mir, Gastric ulcer: an overview, *Int. J. Current Res. Phys. Pharmacol.*, (2023), 1–7. Available from: https://ijcrpp.com/index.php/ijcrpp/article/view/63

8. J. J. Hwang, D. H. Lee, A. R. Lee, H. Yoon, C. M. Shin, Y. Park, et al., Characteristics of gastric cancer in peptic ulcer patients with *Helicobacter pylori* infection, *World J. Gastroentero.*, **21** (2015), 4954. https://doi.org/10.3748/wjg.v21.i16.4954

9. M. Kinyili, J. B. Munyakazi, A. Y. Mukhtar, Modeling the impact of combined use of COVID Alert SA app and vaccination to curb COVID-19 infections in South Africa, *Plos One*, **18** (2023), e0264863. https://doi.org/10.1371/journal.pone.0264863

10. G. K. Mutua, C. G. Ngari, G. G. Muthuri, D. M. Kitavi, Mathematical modeling and simulating of *Helicobacter pylori* treatment and transmission implications on stomach cancer dynamics, *Commun. Math. Biol. Neurosci.*, (2022). https://scik.org/index.php/cmbn/article/view/7542/0

11. T. Feng, Z. Zheng, J. Xu, P. Cao, S. Gao, X. Yu, Cost-effectiveness analysis of the Helico-bacter pylori screening programme in an asymptomatic population in China, *Int. J. Environ. Res. Public Health*, **19** (2022), 9986. https://doi.org/10.3390/ijerph19169986

12. M. Cousins, J. M. Sargeant, D. Fisman, A. L. Greer, Modelling the transmission dynamics of Campylobacter in Ontario, Canada, assuming house flies, Musca domestica, are a mechanical vector of disease transmission, *Royal Soc. Open Sci.*, **6** (2019), 181394. https://doi.org/10.1098/rsos.181394

13. M. P. Dore, D. Y. Graham, Modern approach to the diagnosis of *Helicobacter pylori* infection, *Aliment. Pharm. Therap.*, **55** (2022). https://doi.org/10.1111/apt.16566

14. M. Wameko, P. Koya, A. Wodajo, Mathematical model for transmission dynamics of typhoid fever with optimal control strategies, *Int. J. Indust. Math.*, **12** (2020), 283–296.

15. G. T. Tilahun, O. D. Makinde, D. Malonza, Co-dynamics of pneumonia and typhoid fever diseases with cost effective optimal control analysis, *Appl. Math. Comput.*, **316** (2018), 438–459. https://doi.org/10.1016/jamc.2017.07.063

16. G. T. Tilahun, O. D. Makinde, D. Malonza, Modelling and optimal control of typhoid fever disease with cost-effective strategies, *Comput. Math. Methods Med.*, **2017** (2017), 2324518. https://doi.org/10.1155/2017/2324518

17. P. Duve, S. Charles, J. Munyakazi, R. Lühken, P. Witbooi, A mathematical model for malaria disease dynamics with vaccination and infected immigrants, *Math. Biosci. Eng.*, **21** (2024), 1082–1109. https://doi.org/10.3934/mbe.2024045

18. M. Kinyili, J. B. Munyakazi, A. Y. Mukhtar, To use face masks or not after COVID-19 vaccination? An impact analysis using mathematical modeling, *Front. Appl. Math. Stat.*, **8** (2022), 872284. https://doi.org/10.3389/fams.2022.872284

19. A. Omame, S. A. Iyaniwura, Q. Han, A. Ebenezer, N. L. Bragazzi, et al., Dynamics of Mpox in an HIV endemic community: A mathematical modelling approach, *Math. Biosci. Eng.*, **22** (2025), 225–259. https://doi.org/10.3934/mbe.2025010

20. M. Kinyili, J. B. Munyakazi, A. Y. Mukhtar, Mathematical modeling and impact analysis of the use of COVID Alert SA app, *AIMS Public Health*, **9** (2022), 106–128. https://doi.org/10.3934/publichealth.2022009

21. L. Liu, X. Wang, Y. Li, Mathematical analysis and optimal control of an epidemic model with vaccination and different infectivity, *Math. Biosci. Eng.*, **20** (2023), 20914–20938. https://doi.org/10.3934/mbe.2023925

22. M. Kinyili, J. M-S. Lubuma, J. B. Munyakazi, A. Y. A. Mukhtar, Analyzing the role of comorbidity on COVID-19 infections by mathematical modeling, *J. Math. Comput. Sci.*, **14** (2024). https://scik.org/index.php/jmcs/article/view/7582

23. P. Van den Driessche, J. Watmough, Reproduction numbers and sub-threshold endemic Equilibria for compartmental models of disease transmission, *Math. Biosci.*, **180** (2004), 29–48. https://doi.org/10.1016/S0025-5564(02)00108-6

24. C. Castillo-Chavez, B. Song, Dynamical models of tuberculosis and their applications, *Math. Biosci. Eng.*, **1** (2004), 361–404. https://doi.org/10.3934/mbe.2004.1.361

25. T. J. Tsafack, C. K. Kum, A. J. O. Tassé, B. Tsanou, Mathematical modelling of the dynamics of typhoid fever and two modes of treatment in a Health District in Cameroon, *Math. Biosci. Eng.*, **22** (2025), 477–510. https://doi.org/10.3934/mbe.2025018

26. M. F. T. Rupnow, R. D. Shachter, D. K. Owens, J. Parsonnet, A dynamic transmission model for predicting trends in Helicobacter pylori and associated diseases in the United States, *Emerg. Infect. Diseases*, **6** (2000), 228–237. https://doi.org/10.3201/eid0603.000302

27. Q. Chen, X. Liang, X. Long, L. Yu, W. Liu, H. Lu, Cost effectiveness analysis of screen and treat strategy in asymptomatic Chinese for preventing *Helicobacter pylori* associated diseases, *Helicobacter*, **24** (2019), e12563. https://doi.org/10.1111/hel.12563

28. Y. C. Lee, T. H. Chiang, H. M. Chiu, W. W. Su, K. C. Chou, S. L. S. Chen, et al., Screening for *Helicobacter pylori* to prevent gastric cancer: A pragmatic randomized clinical trial, *JAMA*, **332** (2024), 1642–1651. https://doi.org/10.1001/jama.2024.14887

29. K. F. Pan, L. Zhang, M. Gerhard, J. L. Ma, W. D. Liu, K. Ulm, et al., A large randomised controlled intervention trial to prevent gastric cancer by eradication of *Helicobacter pylori* in Linqu County, China: Baseline results and factors affecting the eradication, *Gut*, **65** (2016), 9–18. https://doi.org/10.1136/gutjnl-2015-309197

30. S. Take, M. Mizuno, K. Ishiki, C. Kusumoto, T. Imada, F. Hamada, et al., Correction to: Risk of gastric cancer in the second decade of follow-up after *Helicobacter pylori* eradication, *J. Gastroenterol.*, **55** (2019), 289. https://doi.org/10.1007/s00535-019-01654-x

31. M. Ghosh, P. Chandra, P. Sinha, J. B. Shukla, Modelling the spread of bacterial infectious disease with environmental effect in a logistically growing human population, *Nonlinear Anal. Real World Appl.*, **7** (2006), 341–363. https://doi.org/10.1016/j.nonrwa.2005.03.005

32. G. T. Tilahun, O. D. Makinde, D. Malonza, Modelling and optimal control of pneumonia disease with cost-effective strategies, *J. Biol. Dynam.*, **11** (2017), suppl. 2, 400–426. https://doi.org/10.1080/17513758.2017.1337245

33. V. N. Njenga, C. G. Ngari, W. M. Nduku, L. S. Luboobi, Modelling the impact of hygiene and treatment on the dynamics of childhood diarrhea in Nairobi County, Kenya, *Int. J. Math. Math. Sci.*, (2024), 3336826. https://doi.org/10.1155/2024/3336826

Supplementary

Appendix A

Proof of theorem (3.6).

Proof. Lyapunov functions are used to compute the global asymptotic stability of the endemic equilibrium [15, 32]. The Lyapunov function L is defined as

$$\begin{aligned} L(S^*, E^*, I^*, I_S^*, T^*, I_C^*, B^*) &= \left(S - S^* - S^* ln\frac{S^*}{S}\right) + \left(E - E^* - E^* ln\frac{E^*}{E}\right) \\ &+ \left(I - I^* - I^* ln\frac{I^*}{I}\right) + \left(I_S - I_S^* - I_S^* ln\frac{I_S^*}{I_S}\right) \\ &+ \left(T - T^* - T^* ln\frac{T^*}{T}\right) + \left(I_C - I_C^* - I_C^* ln\frac{I_C^*}{I_C}\right) \\ &+ \left(B - B^* - B^* ln\frac{B^*}{B}\right). \end{aligned} \tag{5.1}$$

Obtaining the derivative of (5.1) with respect to t gives

$$\begin{aligned} \frac{dL}{dt} &= \left(\frac{S - S^*}{S}\right)\frac{dS}{dt} + \left(\frac{E - E^*}{E}\right)\frac{dE}{dt} \\ &+ \left(\frac{I - I^*}{I}\right)\frac{dI}{dt} + \left(\frac{I_S - I_S^*}{I_S}\right)\frac{dI_S}{dt} \\ &+ \left(\frac{T - T^*}{T}\right)\frac{dT}{dt} + \left(\frac{I_C - I_C^*}{I_C}\right)\frac{dI_C}{dt} + \left(\frac{B - B^*}{B}\right)\frac{dB}{dt}. \end{aligned} \tag{5.2}$$

By replacing

$$\frac{dS}{dt}, \frac{dE}{dt}, \frac{dI}{dt}, \frac{dI_S}{dt}, \frac{dT}{dt}, \frac{dI_C}{dt} and \frac{dB}{dt},$$

into the (5.2), we obtain

$$\begin{aligned} \frac{dL}{dt} &= \left(\frac{S - S^*}{S}\right)(\pi + \zeta T - (\lambda + \mu)S) + \left(\frac{E - E^*}{E}\right)(\lambda S - (\omega + \mu + \rho)E) \\ &+ \left(\frac{I - I^*}{I}\right)((1 - \omega)\rho E - (\theta + \alpha + \mu)I) \\ &+ \left(\frac{I_S - I_S^*}{I_S}\right)(\omega E + \theta I - (\mu + \epsilon + \gamma)I_S) \\ &+ \left(\frac{T - T^*}{T}\right)(\epsilon I_S - (\mu + \eta + \zeta)T) + \left(\frac{I_C - I_C^*}{I_C}\right)(\alpha I + \gamma I_S + \eta T - (\mu + \delta)I_C) \end{aligned}$$

$$+\left(\frac{B-B^*}{B}\right)(\sigma_1 I+\sigma_2 I_S+\sigma_3 T+\sigma_4 I_C-\tau B). \tag{5.3}$$

Simplifying (5.3) and collecting positive and negative terms together, we obtained

$$\frac{dL}{dt} = \mathcal{M}-\mathcal{N}, \tag{5.4}$$

where

$$\begin{aligned}\mathcal{M} &= \pi+\zeta T+\frac{\zeta T^*S^*}{S}+\lambda S+\frac{\lambda S^*E^*}{E}+\rho E\\ &+\rho E^*I^*+\omega E+\theta I+\frac{\omega E^*I_S^*}{I_S}+\frac{\theta I I_S^*}{I_S}+\epsilon I_S\\ &+\frac{\epsilon I_S T^*}{T}+\alpha I+\gamma I_S+\eta T+\frac{\alpha I^*I_C^*}{I_C}\\ &+\frac{\gamma I_S^*I_C^*}{I_C}+\frac{\eta T^*I_C^*}{I_C}+\sigma_1 I+\sigma_2 I_S+\sigma_3 T\\ &+\sigma_4 I_C+\frac{\sigma_1 I^*B^*}{B}+\frac{\sigma_2 I_S^*B^*}{B}+\frac{\sigma_3 T^*B^*}{B}+\frac{\sigma_4 I_C^*B^*}{B}.\end{aligned} \tag{5.5}$$

$$\begin{aligned}\mathcal{N} &= \zeta T^*+\frac{\pi S^*}{S}+\frac{\zeta T S^*}{S}+\lambda S^*+\frac{\lambda S E^*}{E}\\ &\rho E^*+\frac{\rho E I^*}{I}+\omega E^*+\theta I^*+\frac{\omega E I_S^*}{I_S}\\ &\epsilon T^*+\frac{\alpha I I_C^*}{I_C}+\frac{\gamma I_S I_C^*}{I_C}+\frac{\eta T I_C^*}{I_C}+\sigma_1 I^*+\sigma_2 I_S^*\\ &+\sigma_3 T^*+\sigma_4 I_C^*+\frac{\sigma_1 I B^*}{B}+\frac{\sigma_2 I_S B^*}{B}+\frac{\sigma_3 T B^*}{B}+\frac{\sigma_4 I_C B^*}{B}\\ &+[\lambda+\mu]\frac{(S-S^*)^2}{S}+[\omega+\mu+\rho]\frac{(E-E^*)^2}{E}\\ &+[\theta+\alpha+\mu]\frac{(I-I^*)^2}{I}+[\mu+\epsilon+\gamma]\frac{\left(I_S-I_S^*\right)^2}{I_S}\\ &[\mu+\eta+\zeta]\frac{(T-T^*)^2}{T}+[\mu+\delta]\frac{\left(I_C-I_C^*\right)^2}{I_C}+\tau\frac{(B-B^*)^2}{B}.\end{aligned} \tag{5.6}$$

Therefore, if $\mathcal{M}<\mathcal{N}$, then $\frac{dL}{dt}\le 0$.
Note that $\frac{dL}{dt}=0$ if and only if $S=S^*, E=E^*, I=I^*, I_S=I_S^*, T=T^*, I_C=I_C^*$, and $B=B^*$. Thus, the largest compact invariant set

$$(S^*,E^*,I^*,I_S^*,T^*,I_C^*,B^*)\in\Omega:\frac{dL}{dt}=0,$$

is the singleton P^*, where P^* is the endemic equilibrium of the system. By Lasalle's invariant principle [33], it implies that $P^*$is globally asymptotically stable in Ω if $\mathcal{M}<\mathcal{N}$. □

AIMS Press